01 Dec 2008

Using Automated Inclusion Analysis for Casting Process Improvements

Vintee Singh

Semen Naumovich Lekakh
Missouri University of Science and Technology, lekakhs@mst.edu

Kent D. Peaslee
Missouri University of Science and Technology

Using Automated Inclusion Analysis for Casting Process Improvements

Vintee Singh, Simon Lekakh, and Kent Peaslee[a],
Department of Materials Science & Engineering, Missouri University of Science and Technology, Rolla, MO 65409-0330, United States

[a]*Corresponding author: Ph: (573) 341-4714; Fax: (573) 341-6934; E-Mail: kpeaslee@mst.edu*

ABSTRACT

Different industrial melting and ladle practices (deoxidation, slag, refractory types, etc.) used in steel foundries were analyzed and compared using an ASPEX automated inclusion analyzer for study of inclusions. The effects of deoxidation and pouring practices on the size, type and number of inclusions were evaluated for steel foundries equipped with induction and arc melting furnaces, with capacities ranging from 1 to 20 tons. Samples were collected from the furnace, ladle, and castings. Specific rules were developed for classification of inclusions by composition, size distribution and shape. Inclusion statistics, including composition, quantity, shape, and size during cast steel processing from the furnace to the final casting were used for treatment optimization in the foundry ladles.

INTRODUCTION

The toughness of steel is very important in many critical applications where fracture resulting in failure could produce catastrophic effects. The toughness of steel depends on the number, size, shape and composition of non-metallic inclusions in the steel matrix. Hence, exact determination of the characteristics of non-metallic inclusions is essential to the success of research aimed at increasing toughness of steel parts.

In a steel part, several types of second phase particles are present including non-metallic inclusions, carbides and nitrides. As illustrated in Figure 1, fracture of steel is due to the growth and coalescence of voids nucleated at some of these second-phase particles. In steel, non-metallic inclusions are the primary particles at which void nucleation occurs. Voids are nucleated at one of these second-phase particles, either by decohesion of the particle-matrix interface or by particle fracture. The voids nucleated at the particles grow until they coalesce by impingement or by the process of void sheet coalescence.[1] Void sheet coalescence requires fracture of the ligament between the voids created at the larger non-metallic inclusions.

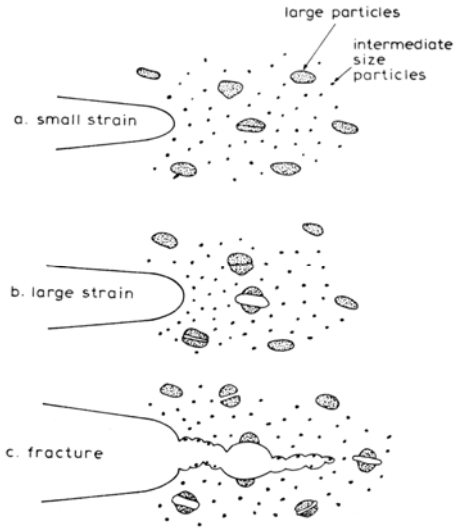

Figure 1: Nucleation of voids on primary inclusions (a, b) and fracture of steel (c)[1]

Recent research has shown that decreasing the volume fraction of inclusions that induce void nucleation and increasing the inclusion spacing result in significant improvement in toughness.[2] The majority of the inclusions in steel are the product of the deoxidation process or reoxidation during pouring and casting solidification. The aim of deoxidation or "killing" is to reduce the dissolved oxygen content of the steel. As the steel solidifies, oxygen dissolved in the liquid cannot be accommodated by the solid crystal structure and therefore reacts with dissolved carbon forming CO gas most of which is trapped in the casting as porosity or pinholes. To avoid porosity, additions are made to the liquid steel to form solid deoxidation products that can be

floated to the surface and removed. However, some of the inclusions (especially smaller and slow floating particles) are trapped in the steel casting as inclusions. Many of the inclusions in castings are also formed by reoxidation in which liquid steel picks up oxygen from contact with the air during pouring and transport through the gating system. In addition, inclusions can be formed by reaction of the liquid steel with water vaporizing from the molding sands and debris in the gating system.

Elements used for deoxidation are those that have a greater affinity for oxygen than carbon and form thermodynamically more stable oxides than iron oxide. These elements include aluminum, silicon, manganese, calcium, zirconium, titanium, magnesium, boron and rare earth metals (REM). Figure 2 summarizes the deoxidation effects of the common deoxidizers:

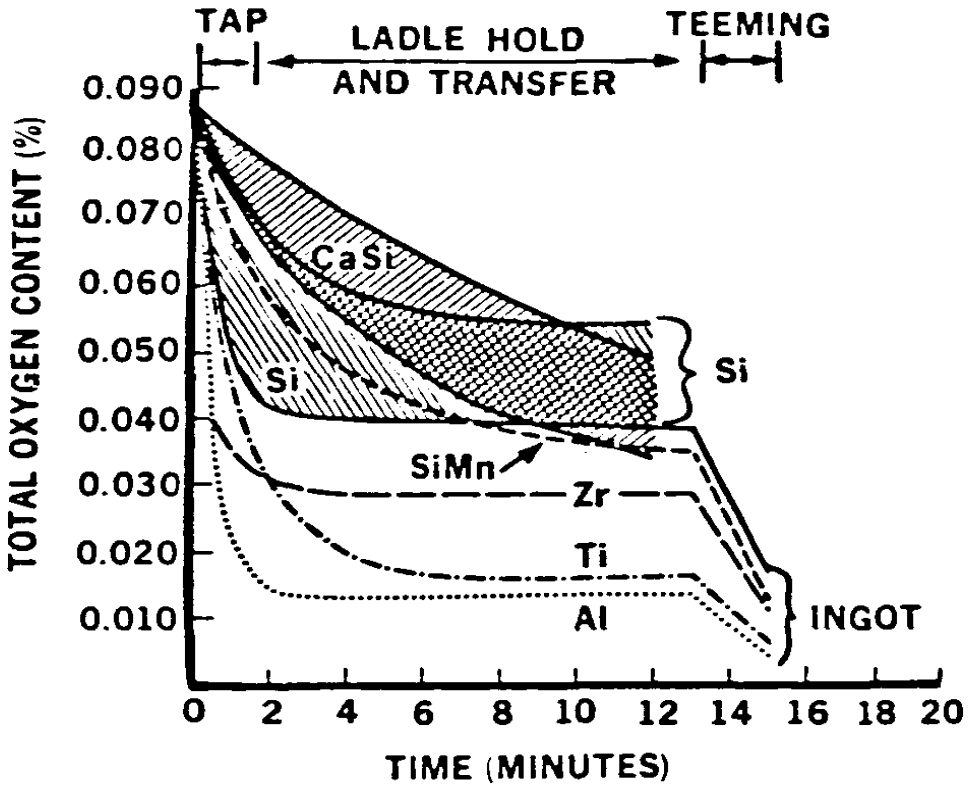

Figure 2: Deoxidation results of the common deoxidizers[3]

The most common deoxidation practice utilized for steel castings is the use of aluminum, which produces solid particles of Al_2O_3. The coalescence of these particles forms aggregates of irregular shape called 'alumina clusters'. They significantly affect the mechanical and fatigue properties of steel, and may also result in the generation of surface defects. One technique used to diminish the harmful effects of Al_2O_3 inclusions is calcium treatment. The addition of calcium promotes partial reduction of the Al_2O_3 inclusions, giving rise to the formation of liquid calcium aluminates with low melting point and spherical morphology, which can easily float out. Most of these liquid inclusions separate easily from the melt, and those not removed are less harmful to the mechanical properties of the final steel product. The reaction sequence followed is:

$$Al_2O_3 \rightarrow CA_6 \rightarrow CA_2 \rightarrow CA \rightarrow C_{12}A_7$$

where C and A denote CaO and Al_2O_3, respectively.[4] The CaO- Al_2O_3 phase diagram in Figure 3 shows the presence of CA_2, CA, $C_{12}A_7$ in liquid state at steelmaking temperatures (~ 1650 ^oC).

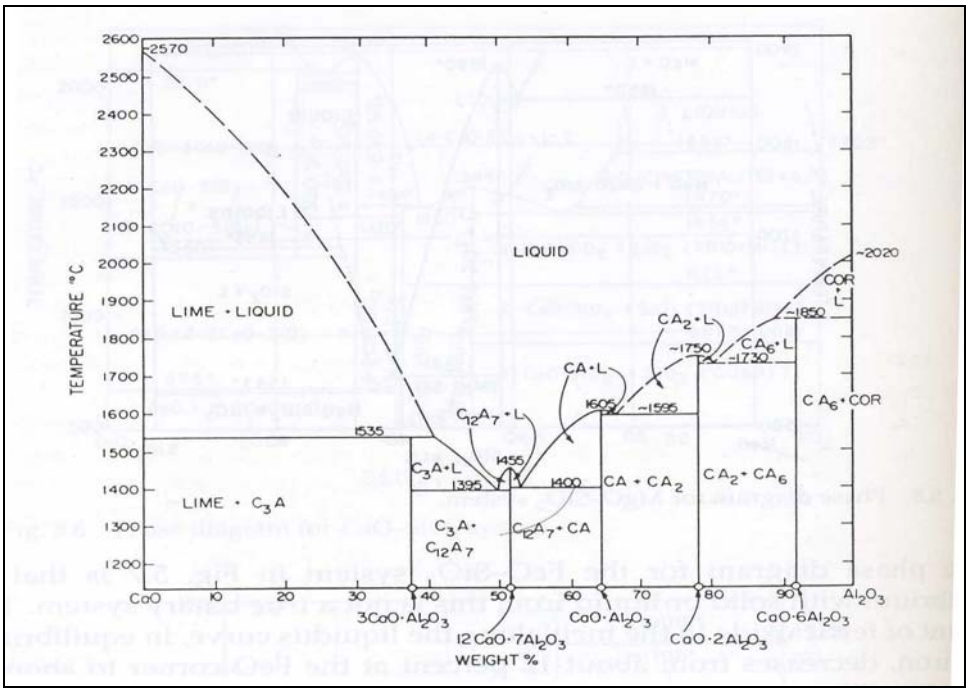

Figure 3: CaO- Al_2O_3 binary phase diagram [5]

As these reactions progress, the activity of Al_2O_3 decreases gradually in the calcium aluminates, allowing more of the Al to react with oxygen, providing even better deoxidation. These inclusions can also react with the sulfur present to form oxy-sulfide inclusions. Sulfide morphology has been classified under Type I, Type II and Type III inclusions, while modified oxy-sulfides have been classified as Type IV inclusions as shown schematically in Table I.[3]

Table I. Different types of sulfides and oxy-sulfides[3]

CLASSIFICATION	OXIDATION STATE	SHAPE OF SULFIDE
Type I	Under Deoxidized ,e.g., Very low soluble Al ,High residual oxygen	Random Large Globules
Type II	Almost Complete Deoxidation, e.g., Low soluble Al, Low residual oxygen	Intergranular Fine Precipitate
Type III	Deoxidation with Excess Deoxidant, e.g., High soluble Al, Very low residual oxygen	Random Large Angular Precipitate
Type IV	As Type III + Ca , RE , etc	Modified Globular

Type II sulfides are to be avoided as they cause a reduction in toughness. Sulfide morphology is not as critical if sulfur is adequately low (<0.010%), but above 0.025% sulfide morphology becomes critical. An aluminum level greater than 0.03 % has been considered a 'safe' chemistry to avoid type II sulfides. However, complex deoxidation reactions, chemistry, local reoxidation, and other unknowns can affect the formation of type II sulfides.[6] Figures 4 and 5 show the effect of chemistry on sulfide morphology, which varies with aluminum content.

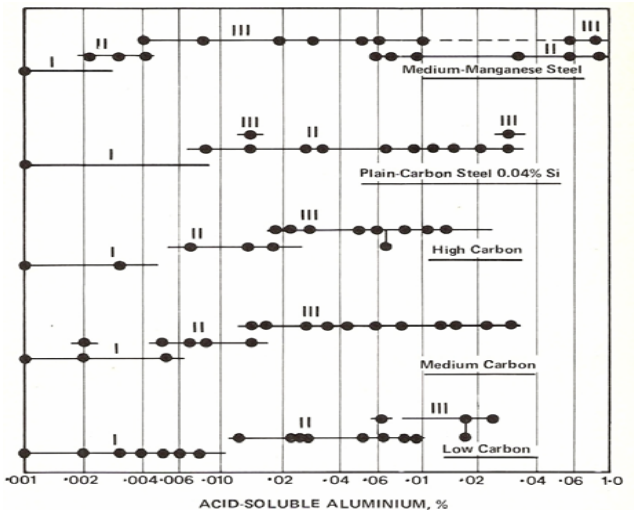

Figure 4: Effect of chemistry on sulfide morphology[7]

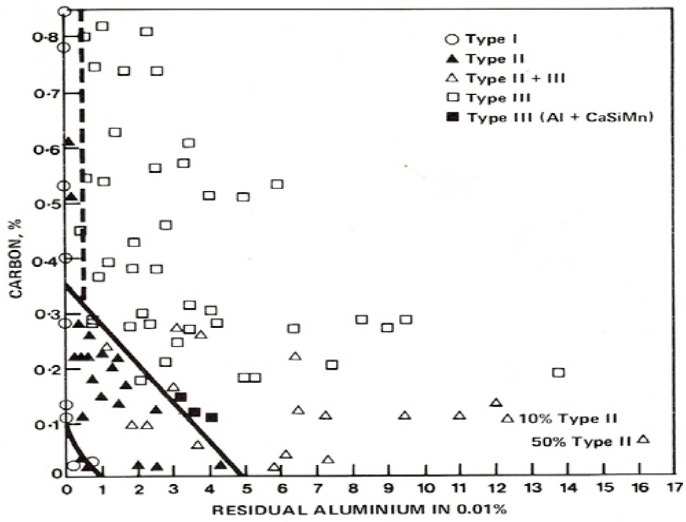

Figure 5: Effect of Carbon and Aluminum on Sulfide Shape[8]

As shown in Figure 6, the actual sulfide shape depends on the type and amount of the deoxidizers added. Such morphology has a significant effect on the resultant mechanical properties of the cast steel product. Therefore, deoxidized steel castings may still suffer from various detrimental mechanical property values due to poor removal of the deoxidation products. Hence the final deoxidation and pouring practices should be such that they control the number, composition and morphology of inclusions present in the steel.

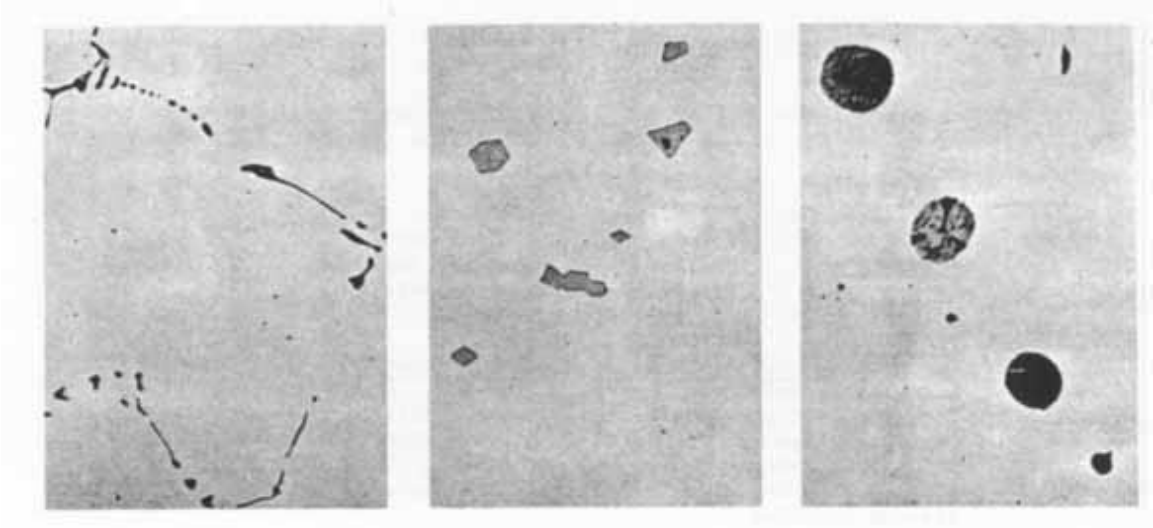

(a) (b) (c)

Figure 6: Sulfide inclusions (a) Type II, 0.009 % Al residual content after deoxidation (b) Type III, 0.03 % residual Al content (c) Type I, Si-killed (all at 500X)**.**[9]

Manual scanning electron microscopy (SEM) analysis combined with energy dispersive spectroscopy (EDS) has been used for inclusion characterization in the past. However, this approach is limited by the intensive nature involved because an SEM operator must analyze individual inclusions, which is time consuming. The system used for this research, ASPEX PICA-1020 (Particle Identification and Characterization Analyzer) provides a rapid and accurate method for determining the type, size, number, and spacing of inclusions present in steel samples. On the other hand, Aspex allows for automated characterization of all the inclusions in a microscopic specimen including the volume fraction, size and shape, inclusion spacing and complete inclusion identification. With the use of this equipment, the possible number of inclusions analyzed could be increased dramatically from the tens to the thousands, while decreasing the total time involved from days to minutes.

EXPERIMENTAL PROCEDURE

Plant trials were conducted at three foundries with different deoxidation practices in the furnace and ladle as summarized in Table II.

Table II. Deoxidation practices at foundries in study

	Charge Wt.	Furnace additions	Ladle additions
Plant A	1000 lbs.	-	Al= 1 lb/ton FeTi= 0.5 lbs/ton FeSiZr= 0.875 lbs/ton
Plant B	1400 lbs.	Al= 0.8 lb/ton	CaSi= 5 lbs/ton added in-stream
Plant C-Acid	40,000 lbs.	FeSi= 0.175 lbs/ton SiMn= 22.425 lbs/ton	CaSi Bar= 1.25 lbs/ton Al= 0.78 lbs/ton CaSi wire= 591 ft
Plant C-Basic	40,000 lbs.	FeSi= 11.35 lbs/ton SiMn= 8.275 lbs/ton	CaSi Bar= 1.28 lbs/ton Al= 0.77 lbs/ton CaSi wire= 466 ft

In the plant trials, the dissolved oxygen content was measured directly in the melt, using Celox oxygen probes and the Celox Lab Datacast-2000. Steel samples were collected from the furnace and the ladle, before and after the addition of deoxidants. In addition, samples were cut from castings produced from the same melt. Microscopic specimens were prepared from these samples and analyzed using the Aspex PICA-1020 and total oxygen content was measured using a Leco TC-500. The measurement of both total and dissolved oxygen is important for understanding the deoxidation process. Total oxygen content includes the oxygen associated with inclusions and soluble or "free" oxygen. Soluble oxygen is the oxygen which is actually in solution and not associated with inclusions. Therefore, the total oxygen is always greater than the oxygen in solution.[10]

In the Aspex SEM system, a focused electron beam is moved across the specimen in an array of fairly coarse steps, as shown in Figure 7. The field is subdivided into smaller fields. For example, a 4X4 mm square sample field can be broken down into 16 fields of 1x1mm square that are defined electronically. That is, the beam is displaced by the scan system so that each 1mm area is treated as a separate field, reducing the number of time-consuming mechanical stage motions sixteen-fold. As the electron beam moves across each field, the brightness or intensity of the BSED or SED signal is recorded and transferred to the computer memory as representing the brightness of a single pixel (Figure 7b). If the signal is bright enough to indicate that an inclusion is present at the position, the software initiates a particle-sizing sequence using a rotating chord algorithm. Once the coarse scanning (indicated by the dots) identifies an inclusion, the center is identified and chords are drawn with the beam on the inclusion to define the size and shape of the inclusion. This is a fast process because the instrument only spends time collecting EDS detailed data where inclusions are known to be present, rather than spending time capturing and analyzing vast numbers of essentially empty pixels. Subsequently a number of size and shape parameters are computed from the lengths of the chords.[11]

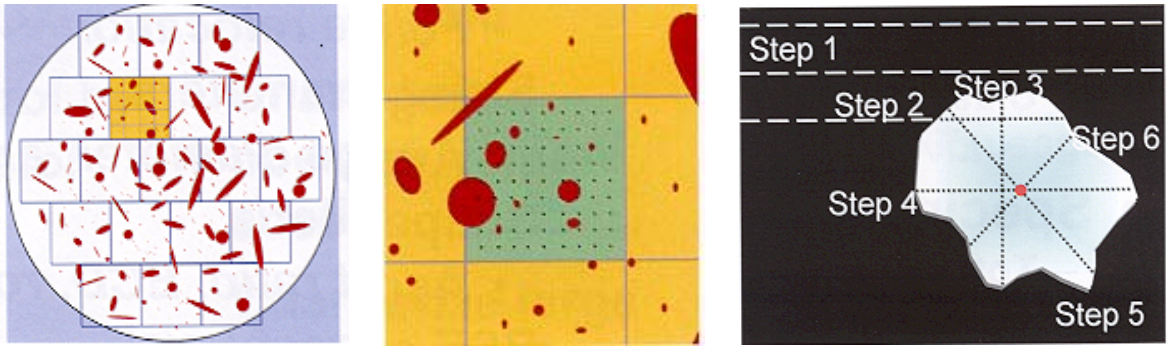

(a) (b) (c)

Figure 7: Automated inclusion analysis including a) subdividing the image into fields, b) moving electron beam across field in an array and c) sizing and cataloging of particles detected by back scattering electrons and centering the beam on each particle and obtaining composition by x-ray spectroscopy[11]

After inclusions have been fully characterized for size and shape, an Energy Dispersive Spectroscopy (EDS) spectrum is acquired to determine the elemental composition of each inclusion. After the sample has been completely analyzed and the data stored, the data is evaluated offline by the Automated Feature Analysis software. The inclusions are classified into various classes based on their composition as determined by user-defined rules. For example, an inclusion with Mn >= 30% and S >=20% is classed as a MnS inclusion.

RESULTS AND DISCUSSION

Plant A

In this study, one induction furnace heat was followed from melting through deoxidation and casting of medium-carbon steel (WBC) in a 1000 lb ladle. Al, FeTi and FeSiZr were added as deoxidants in the ladle. Figure 8 compares the percent area covered by inclusions at the various stages of liquid processing, as measured by the Aspex system. The area and number of inclusions increased after the addition of deoxidants with significant changes in the inclusion composition. The volume of alumina particles increased after aluminum deoxidation in ladle. The volume of TiO_2 inclusions increased in the ladle after the addition of FeTi during tap. The volume of non-metallic inclusions increase during the pour with the final casting having more inclusions than the ladle indicating that there is insufficient time to float inclusions in the ladle and significant reoxidation during pouring and transport through the gating system.

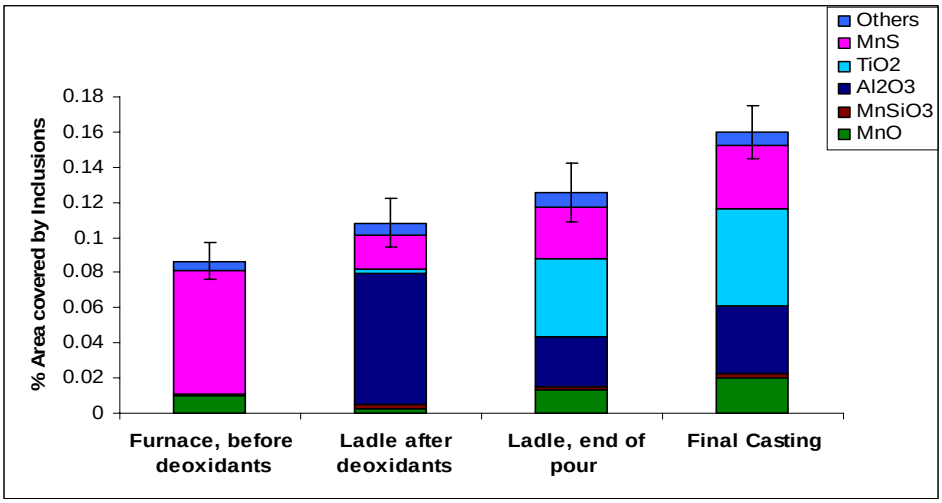

Figure 8: Comparison of inclusion volume in samples collected at various stages of the casting process (Plant A)

Figure 9 shows that the dissolved oxygen dropped after deoxidation, resulting in the formation of a large number of oxide inclusions and an increase in the total oxygen. As the steel processing progressed and the liquid temperature decreased, the oxygen solubility decreased, resulting in lower dissolved oxygen. However, the total oxygen increased during the same period, indicating reoxidation and a lack of inclusion flotation. This is in agreement with the ASPEX inclusion analysis in Figure 8.

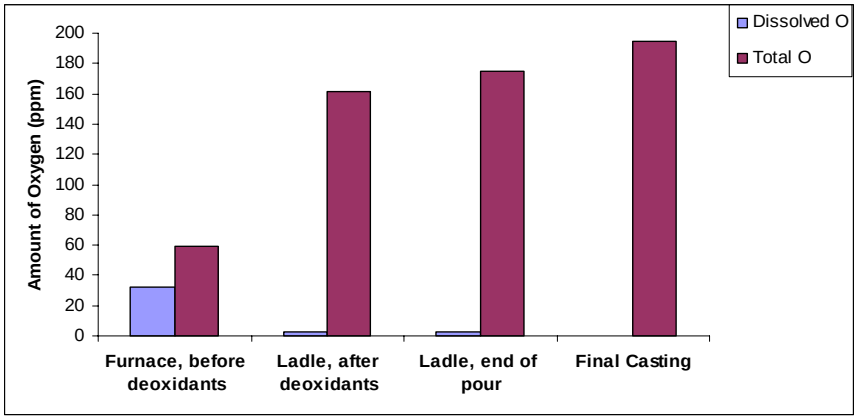

Figure 9: Dissolved and total oxygen measured in samples collected at various stages of the casting process (Plant A)

Plant B

In the trial at Plant B, a heat of medium-carbon steel (8625 alloy) was melted in an induction furnace and tapped into a 1400 lb capacity ladle. For deoxidation, aluminum was added in the furnace just before tap, followed by a calcium silicon addition in the tap stream. Figures 10 and 11 show the percent area covered by inclusions and the dissolved and total oxygen, for samples collected during various stages of the casting process. Figures 12 and 13 show the ternary plots for sulfides and oxides, before and after Ca addition in the ladle. The region where calcium aluminates (CA) would be present in the ternary are marked with a semi-circle for the oxides.

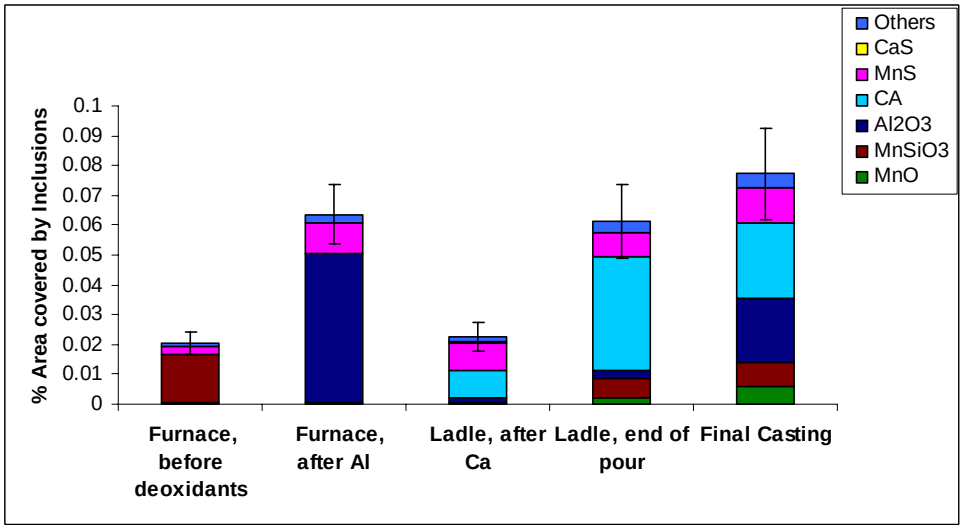

Figure 10: Inclusion area in samples collected at various stages of the casting process (Plant B).

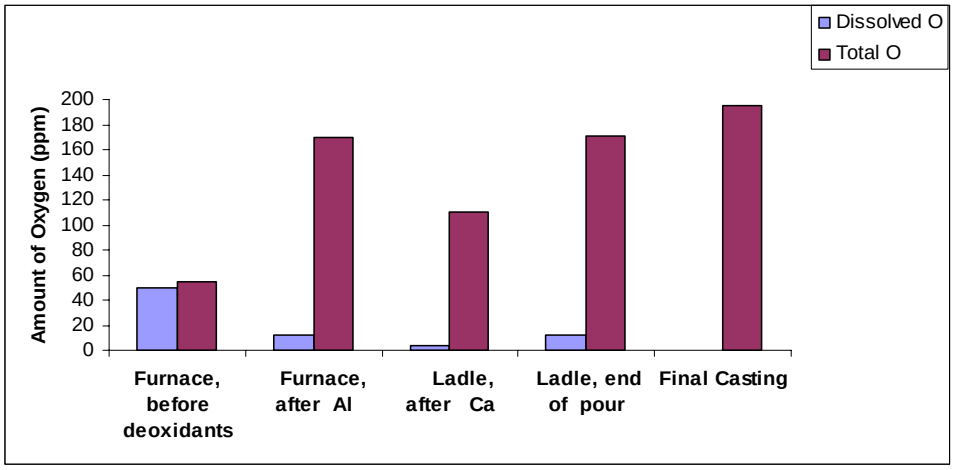

Figure 11: Dissolved and total oxygen measured in samples collected at various stages of the casting process (Plant B).

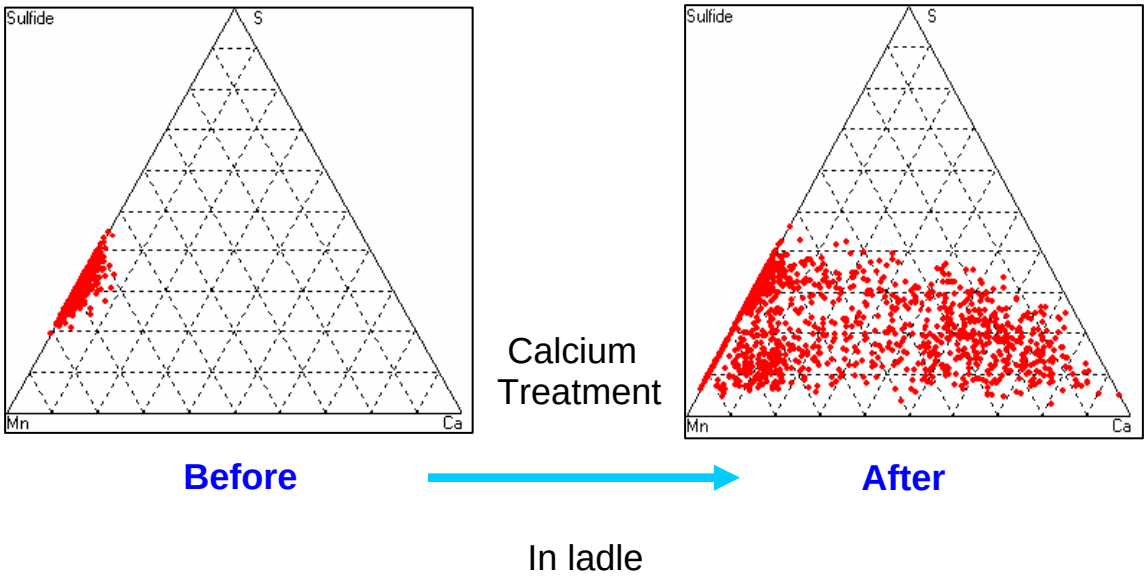

Figure 12: Ternary Mn-Ca-S diagram for casting process, before and after addition of Ca in ladle (Plant B).

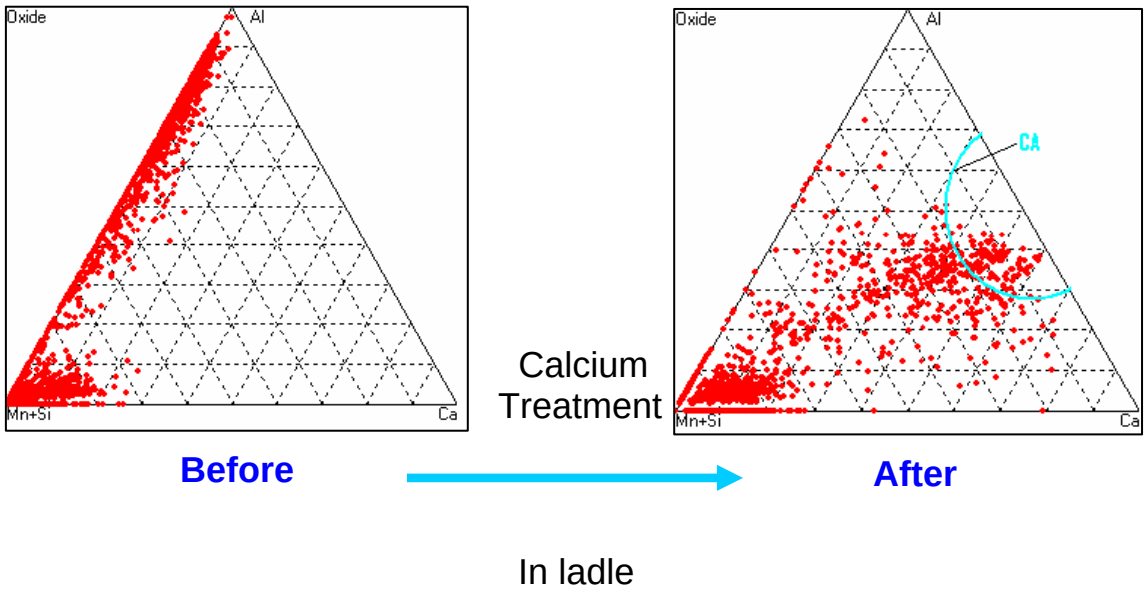

Figure 13: Ternary (Mn+Si)-Ca-Al diagram for casting process, before and after addition of Ca in ladle (Plant B).

The inclusions in the furnace before deoxidation were present as MnS and complex oxides containing Mn and Si. After Al treatment in the furnace, there was an increase in MnS and alumina inclusions and a significant increase in the total oxygen too. The composition and number of inclusions changed after the Ca treatment in the ladle with most of the alumina inclusions forming calcium aluminates (CA). But unmodified alumina and modified CA inclusions increase towards the end of the pour, most likely caused by reoxidation in the casting process, with insufficient flotation.

Contrary to the Ca modification of the alumina inclusions, there was limited Ca modification of the MnS inclusions (Refer the ternary Mn-Ca-S diagram in Figure 12). Adding Ca in the form of CaSi during tap is inconsistent in its metallurgical effectiveness. CaSi was observed to float on the melt surface often flashing indicating vaporization of Ca followed by rapid combustion in air. Ca is highly volatile with a boiling point of 1500 ^{o}C making it difficult to add to the steel without losing it to vaporization. Injection of calcium below the surface of the steel through wire or powder injection would be more effective as it suppresses Ca boiling because of the higher ferrostatic pressure .[12]

Plant C

In Plant C, heats were studied from electric arc furnaces (EAF) utilizing both the acid refractory/slag practice and the basic refractory/slag practice. Ladle treatment included preliminary deoxidation followed by treatment with Ca wire in the ladle. All heats were of a medium-carbon steel with a ladle of capacity 20 tons. During the heat, chemistry samples, slag samples, and dissolved oxygen readings were collected at the following places:

1. Furnace after block
2. Ladle before calcium wire treatment
3. Ladle after calcium wire treatment
4. Ladle at mid ladle pouring

Figures 14 and 15 show the percent area covered by inclusions and dissolved and total oxygen, for both acid and basic processes. In the acid process, the volume of inclusions decreases after addition of the Ca due to the formation of calcium aluminates (CA). Overall, the acid process had significantly more inclusions than the basic process, which is supported by the higher levels of total oxygen. At the same time, the volume of the inclusions remained constant in the basic process.

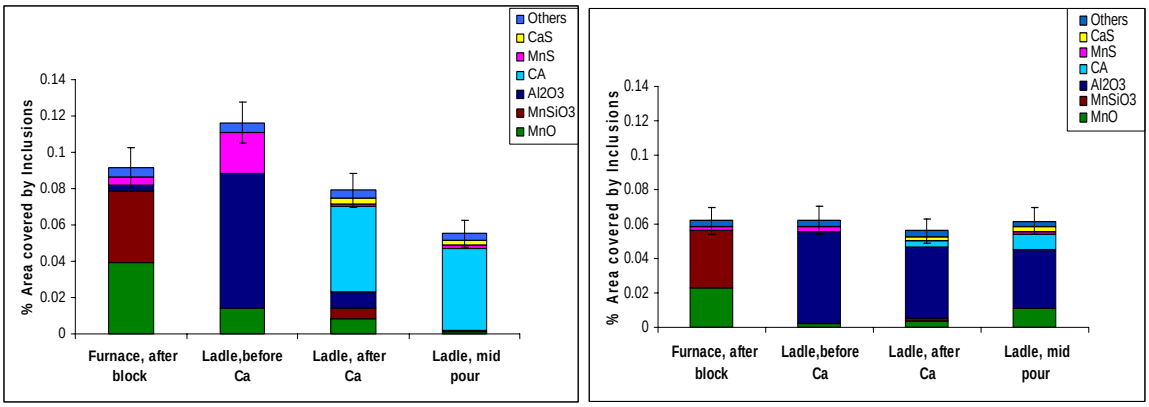

(a) (b)

Figure 14: Inclusion area in samples collected at various stages of the casting process for a) acid and (b) basic process (Plant C).

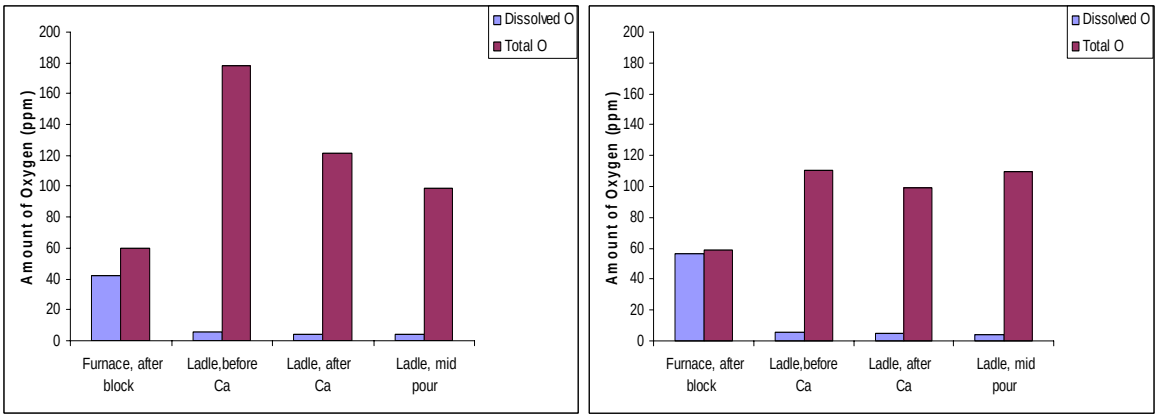

(a) (b)

Figure 15: Dissolved and total oxygen measured in samples collected at various stages of the casting process for (a) acid and (b) basic process (Plant C).

Figure 16 shows Aspex images of manganese sulfide, alumina and CA inclusions, which verify the desired globular morphology of CaS inclusions and higher aspect ratio of alumina and MnS inclusions.

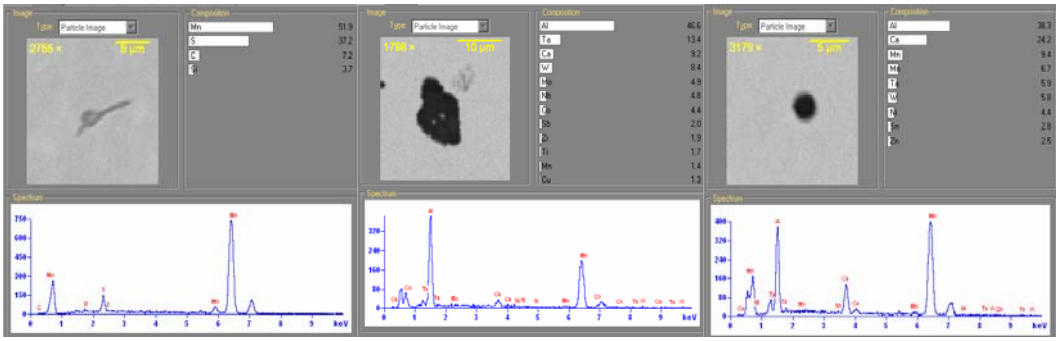

(a) (b) (c)

Figure 16: Aspex images of (a) MnS, (b) Alumina, and (c) CA inclusions.

Figures 17 and 18 summarize the inclusion composition using a ternary composition system for sulfides and oxides, respectively, for the acid process. After the Ca-addition, some of the MnS inclusions are modified to CaS inclusions, which are desired due to its globular morphology. Also, significant amount of CA formation is observed in the acid process, with a decrease in both MnO and Al_2O_3 inclusions. Figure 19 presents a binary phase MnS-CaS diagram, which shows that MnS and CaS could form solid solution above 1150 ^{o}C. This transformation of MnS to MnS-CaS solutions and relatively pure CaS was also observed in the ternary Mn-Ca-S inclusion diagrams.

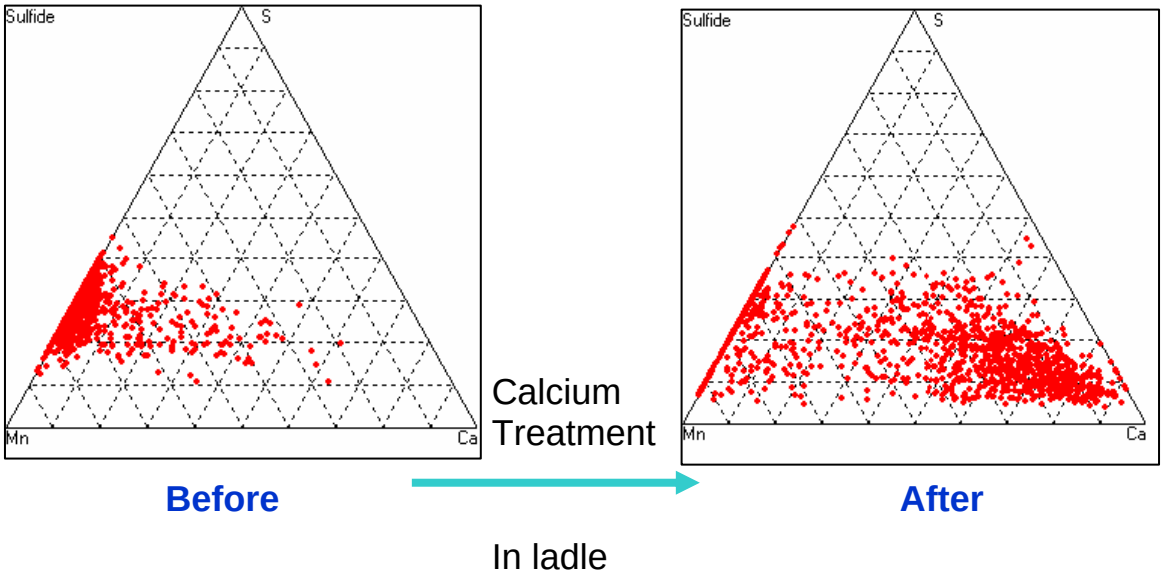

Figure 17: Mn-Ca-S composition diagram for inclusions in acid process before and after addition of Ca in ladle (Plant C).

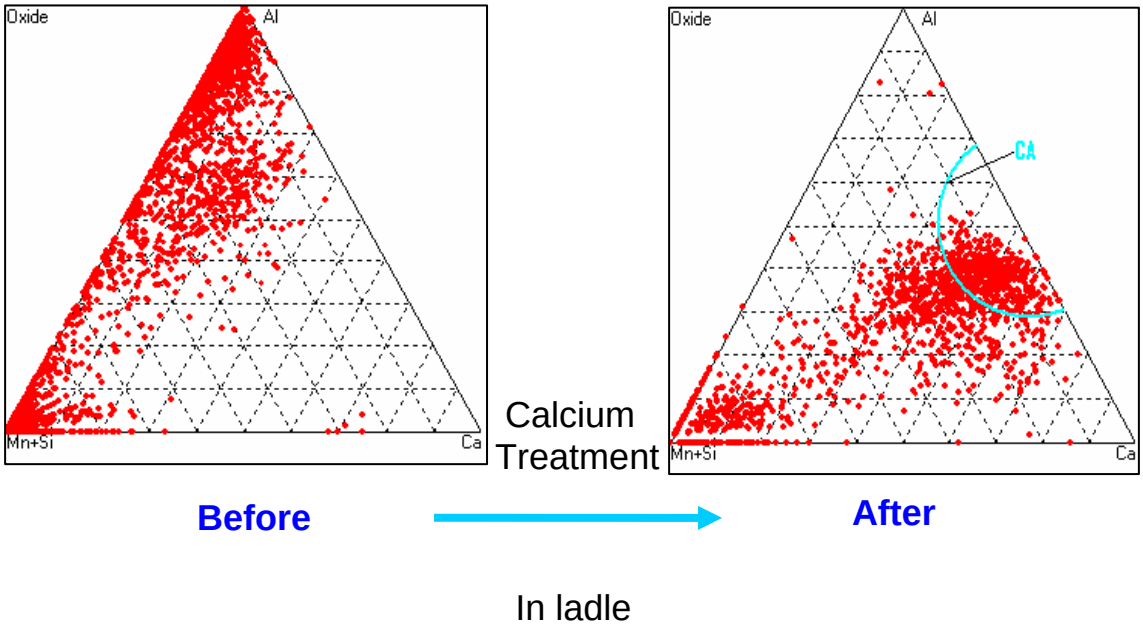

Figure 18: (Mn+Si)-Ca-Al composition of inclusion for acid process, before and after addition of Ca in ladle (Plant C).

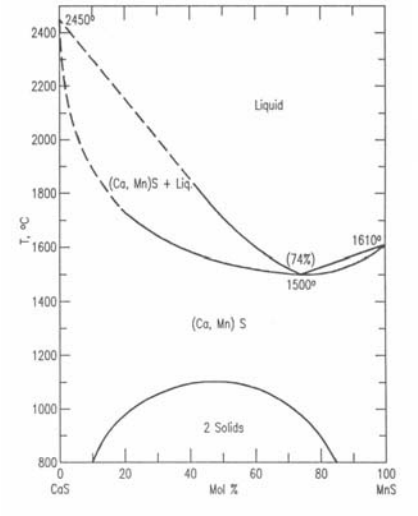

Figure 19: Binary MnS-CaS phase diagram[13]

Figures 20 and 21 show the composition of the sulfide and oxide inclusions for the basic process. Contrary to the acid practice, there was not much decrease in MnS and Al_2O_3 inclusions in the basic practice. Also significant formation of the desired CaS or CA inclusions was not observed in the diagrams for the basic process. The Ca-addition is more beneficial for acid process than the basic process. More CaSi wire was added to the ladle in the acid process (591 ft. in 21 tons) as compared to the basic process (466 ft. in 20 tons). From this study, it can be concluded that the amount of Ca in the basic process was not sufficient to cause the modification of MnS and alumina inclusions.

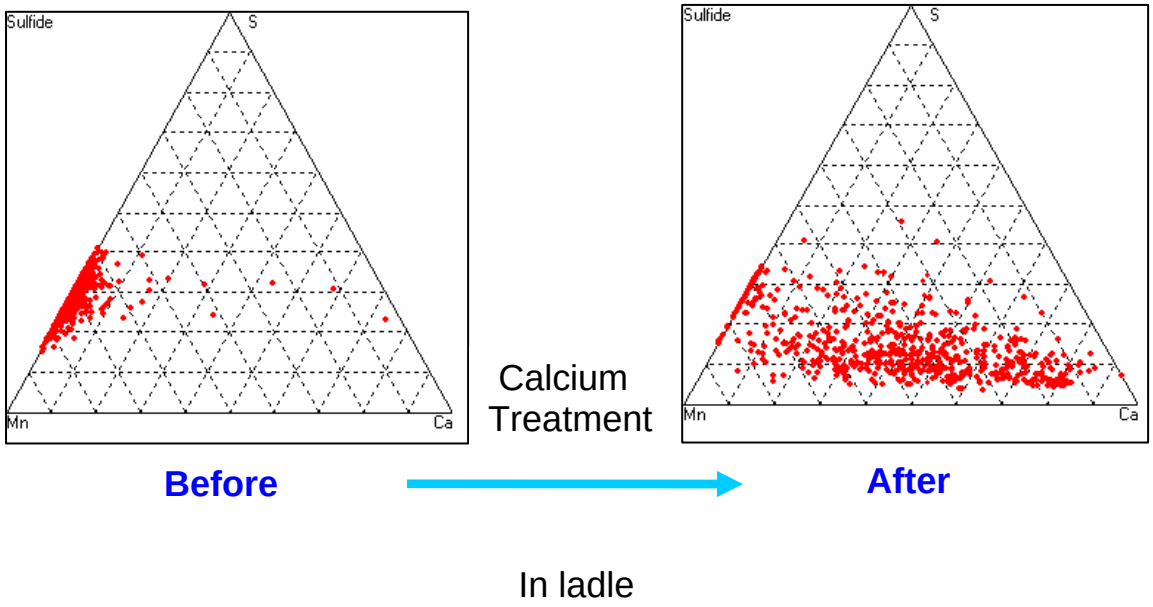

Figure 20: Mn-Ca-S composition of inclusions for basic process, before and after addition of Ca in ladle (Plant C).

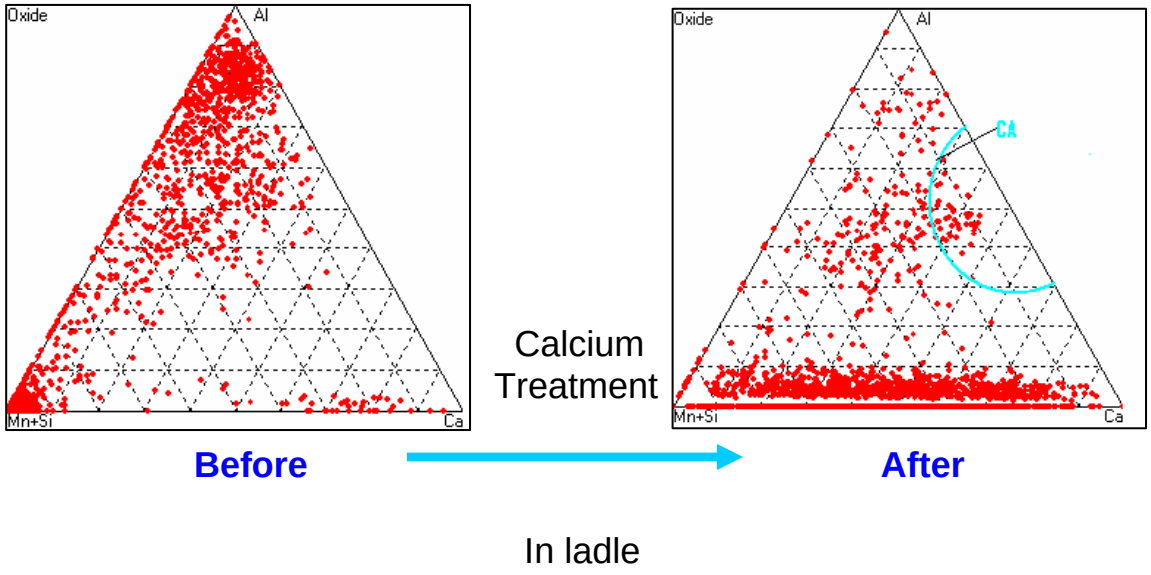

Figure 21: (Mn+Si)-Ca-Al composition of inclusions for basic process, before and after addition of Ca in ladle (Plant C).

In addition to the inclusion analysis, the slag compositions during the various stages of the casting, for both the acid and basic process, were also analyzed (refer Figure 22). The changes observed in the slag chemistry (Fe, P, and S) during the different stages of the casting process, for both acid and basic practices, were plotted in Figure 23. In both the cases, the Fe and P content in slag decreases and the S concentration increases during casting from the furnace to the ladle. At

the same time, basic slag had a lower Fe content and a much larger ability to absorb S as compared to the acid slag. The P concentration for basic steel was lower than acid slags because in the basic furnace practice, slag was removed from the furnace during oxygen blowing. In the acid practice, the slag formed in the furnace was tapped with the heat.

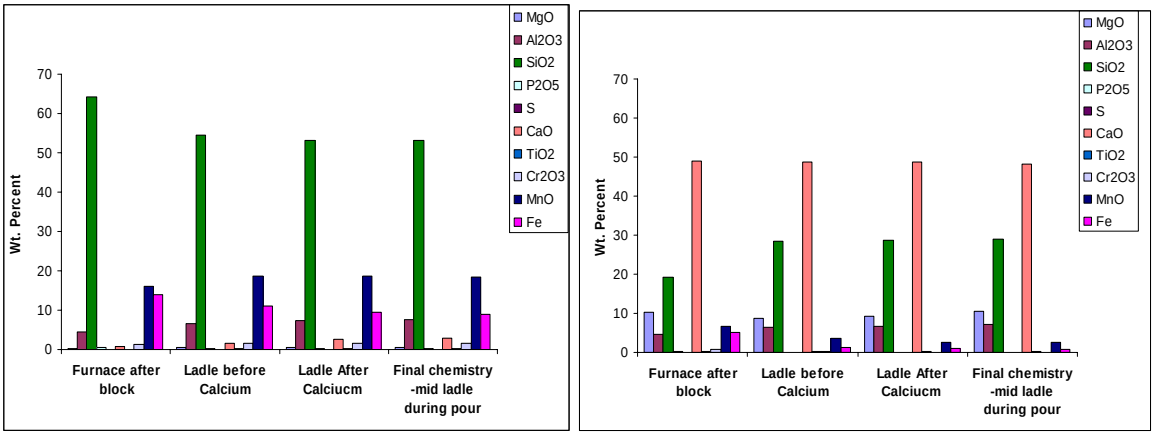

(a) (b)

Figure 22: Slag chemistry for (a) acid and (b) basic process (Plant C).

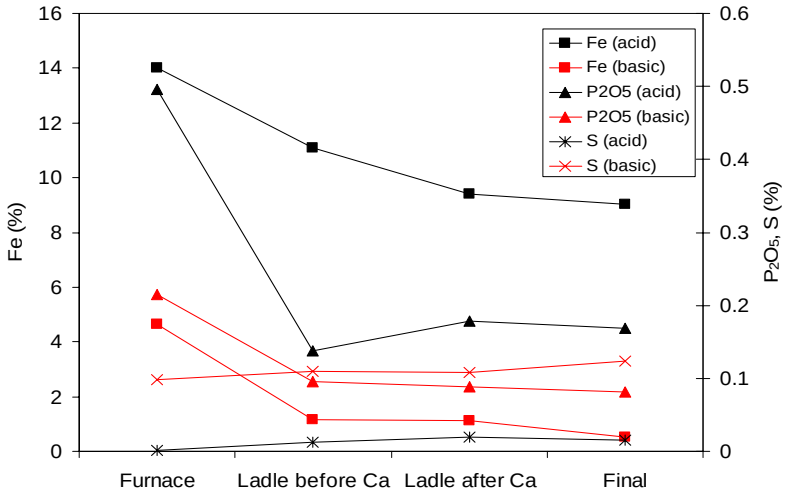

Figure 23: Changing slag chemistry during heats in EAF with acid and basic linings (Plant C).

Based on the slag and metal chemistry for the basic process, the equilibrium S and P partition ratio (% in slag/ % in steel) were calculated using the commercial FACTSAGE software and compared with the measured values (refer Figure 24).The actual results followed similar trends to the calculated values; however the actual slag absorbed much less P than at equilibrium, at the higher iron levels, in the furnace.

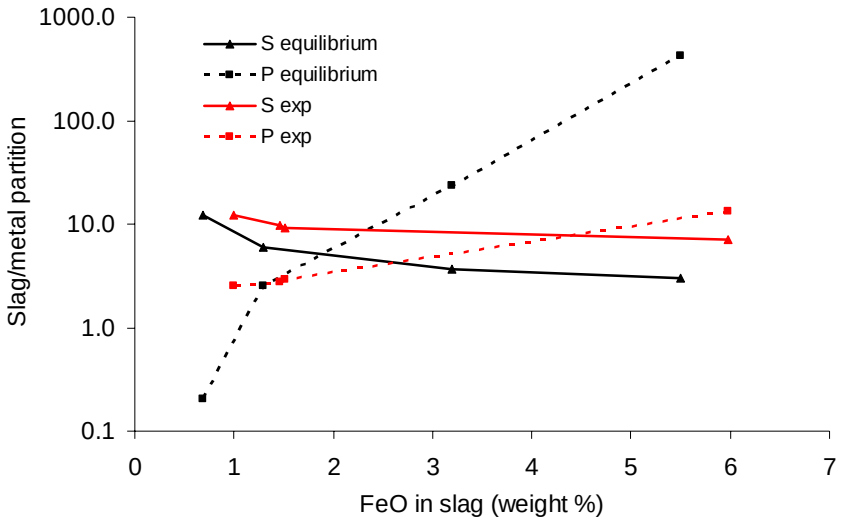

Figure 24: Calculated equilibrium (FACTSAGE) and experimental partition of S and P between slag and melt in basic melting

In addition to the trial heats, casting cleanliness was evaluated for samples from five different basic and acid heats to evaluate the variation between heats. Figures 25 and 26 compare the volume of inclusions per unit area and the total oxygen measured for the samples cut from the ends of the tensile bars, which were poured at mid-heat. The samples from the heats produced by the acid process show a higher level of inclusions when compared to heats produced by the basic process. A significant percentage of these inclusions were MnS inclusions, due to incapability of the acid process to remove S from the slag. The basic process showed many more alumina inclusions in the castings. This is further evidence that the standard Ca-addition is not sufficient to modify alumina inclusions to CA inclusions in the basic process. The total oxygen was higher for basic samples because many of the oxygen containing inclusions, especially alumina, were trapped and not floated out.

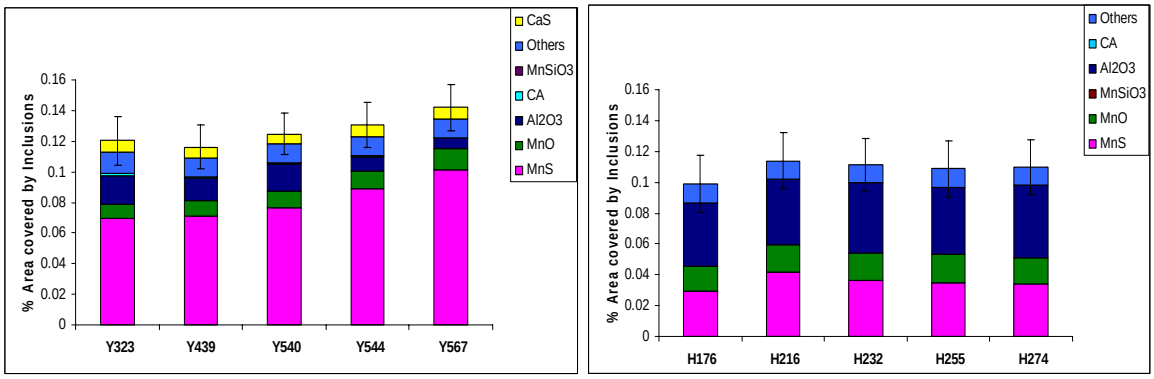

(a) (b)

Figure 25: Inclusion area covered in samples cut from castings from (a) 5 different acid and (b) 5 different basic heats (Plant C).

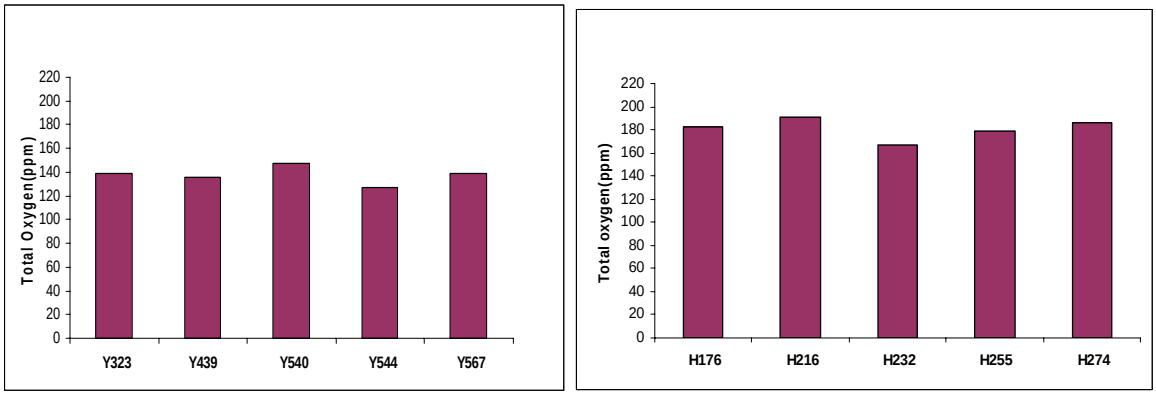

(a) (b)

Figure 26: Total oxygen measured in samples cut from the castings for (a) 5 different acid and (b) 5 different basic heats (Plant C)

Accuracy

Each sample was analysed on the Aspex 3 to 5 times, in order to check the accuracy of the inclusion measurements within a single sample. All the figures which show the percent area covered by inclusions have error bars included. The error bars show little variation from the average data making the ASPEX a reproducible tool for analyses of inclusions.

CONCLUSIONS

This study used a new tool, ASPEX PICA-1020 (Particle Identification and Characterization Analyzer), to characterize, measure and compare non-metallic inclusion transformation during the melting and treatment of cast steels in foundries. Automatic non-metallic inclusion analysis provides an efficient and fast way to analyze the number, shape and composition of the inclusions in cast steel. Deoxidation is essential for steelmaking, but the choice of deoxidizers, melting and ladle practices can minimize the harmful effects of deoxidation products and the presence of inclusions in the cast steel. For example, calcium added in the ladle through wire feeding was beneficial and converted many of the MnS inclusions to CaS inclusions with a globular morphology which is less harmful to physical properties and performance. Also, calcium wire injection is effective in converting alumina inclusions into CA inclusions with lower melting point and spherical morphology enabling their floating and making cleaner steel. However, the calcium addition can only be effective if it is injected in the form of calcium wire below the surface of steel in sufficient quantities, otherwise most of it will vaporize without reacting with the steel melt.

ACKNOWLEDGEMENTS

The work for this project was made available through funding provided by U.S. Army Benet Labs Award W15QKN-07-2-0004 and the funding for the ASPEX inclusion analyzer was made available through U.S. Army DURIP Grant W911NF-08-1-0267. The authors also acknowledge the support of the Steel Founders Society of America and the member companies that participated in this research.

REFERENCES

1. T. B. Cox and Low, J.R., "Investigation of the Plastic Fracture of AISI 4340 and 18 Ni-200 Grade Maraging Steels", Met Trans A, 5A, 1457-1470 (1974).
2. W.M. Garrison, "Controlling Inclusion Distributions to Achieve High Toughness in steels", AIST Trans, 4(5), 132-139 (2007).
3. Moore and Bodor, "Steel deoxidation practice: Special emphasis on heavy section steel castings", AFS Transactions, 93, 99-114 (1985).
4. Herrera et al, "Modification of Al_2O_3 inclusions in medium carbon aluminum steels by AlCaFe additions", Ironmaking and Steelmaking, 33(1 51), (2006).
5. E.T. Turkdogan, Fundamentals of steelmaking (1996).
6. B. Allyn, J. Carpenter, and B. Hanquist, "Deoxidation in Heavy Section Steel Castings", Harrison Steel Castings Company, SFSA Technical and Operating Conference (2006).
7. W. Jackson, "Steelmaking for Steel Founders", SCRATA, January (1977).
8. P. Wieser, "Deoxidation of Steel for Steel Castings", Steel Foundry Facts, February (1970).
9. R. Monroe and J. Svoboda, "Making Quality Steel Castings: A Review of 20 Years of SFSA Literature", SFSA Special Report # 23, (1984).
10. M. Blair, "Review of Deoxidation Practice", SFSA Special Report #25, March (1990).
11. F. H. Schamber and C.G. Van Beek, "Understanding Particulate Contaminants via Automated Electron Beam Analysis", Aspex Corporation (2003).
12. The Making, Shaping and Treating of Steel, Association of Iron and Steel Engineers, (1985).
13. Ernest M. Levin, Carl. R. Robbins, Howard F. McMurdie, Phase diagrams for Ceramists (1983).

.